

Hedgehog signal activates AMPK via Smoothened to promote autophagy and lipid degradation in hepatocytes

Yixing Yao^{a,b}, Tianyuan Li^a, Tingting Yu^a, Xin Yang^a, Yue Wang^a, Jing Cai^a, Steven Y. Cheng^{a,c}, Chen Liu^{a,c}, and Shen Yue^{a,c}

^aDepartment of Medical Genetics, Nanjing Medical University, Nanjing 211166, China; ^bDepartment of Pathology, Suzhou Ninth People's Hospital, Suzhou 215200, China; ^cJiangsu Key Lab of Cancer Biomarkers, Prevention and Treatment, Collaborative Innovation Center for Cancer Personalized Medicine, Nanjing Medical University, Nanjing 211166, China

Corresponding authors: **Steven Y. Cheng** (email: sycheng@njmu.edu.cn); **Chen Liu** (email: liuchen@njmu.edu.cn); **Shen Yue** (email: yueshen@njmu.edu.cn).

Abstract

Studies in the past decade have shown that lipid droplets stored in liver cells under starvation are encapsulated by autophagosomes and fused to lysosomes via the endocytic system. Autophagy responds to a variety of environmental factors inside and outside the cell, so it has a complex signal regulation network. To this end, we first explored the role of Hedgehog (Hh) in autophagy and lipid metabolism. Treatment of normal mouse liver cells with SAG and GDC-0449 revealed elevated phosphorylation of AMP-activated protein kinase (AMPK) and increased lipidation of LC3. SAG, and GDC-0449 were agonist and antagonist of Smoothened (Smo) in canonical Hh pathway, respectively, but they played a consistent role in the regulation of autophagy in hepatocytes. Moreover, SAG and GDC-0449 did not affect the expression of glioma-associated oncogene (Gli1) and patched 1, suggesting the absence of canonical Hh signaling in hepatocytes. We further knocked down the Smo and found that the effects of SAG and GDC-0449 disappeared, indicating that the non-canonical Smo pathway was involved in the regulation of autophagy in hepatocytes. In addition, SAG and GDC-0449 promoted lipid degradation and inhibited lipid production signals. Knockdown of Smo slowed down the rate of lipid degradation rather than Sufu or Gli1, indicating that Hh signaling regulated the lipid metabolism via Smo. In summary, activates AMPK via Smo to promote autophagy and lipid degradation.

Key words: Hh signaling, Smo, AMPK, autophagy, lipid degradation

Introduction

Hedgehog (Hh) signaling, which was first identified in *Drosophila*, plays a vital role in embryonic development and adult stem cell self-renewal (Nusslein-Volhard and Wieschaus 1980; Ingham and McMahon 2001; Lum and Beachy 2004). Its dysfunction has been implicated in various types of cancer and birth defects (Jiang and Hui 2008; Ingham et al. 2011). Canonical activation of Hh signaling starts from the binding of Hh ligand to its receptor patched 1 (Ptch1), which releases G protein-coupled receptor Smoothened (Smo), causing the activation of the glioma-associated oncogene (Gli) transcription factors (Kinzler et al. 1988; Corbit et al. 2005; Rohatgi et al. 2007; Falkenstein and Vokes 2014). Other than canonical pathway, one non-canonical Hh signaling pathway mode refers to activation of downstream of Smo through Gli-independent mechanisms (Riobo et al. 2006; Qu et al. 2013; Praktiknjo et al. 2018). In recent decades, non-canonical Smo pathway involved in different zones of metabolic homeostasis has been reported each year, just like Teperino et al. (2012) found that Smo stimulates insulin-independent glucose uptake in mature 3T3L1 adipocytes via AMP-activated protein kinase (AMPK), which does not require Gli transcriptional activity.

Autophagy, which is a highly conserved recycling process of cellular components, including organelles, proteins, and macromolecules, is similarly reported to be in correlation with metabolic homeostasis (Takeshige et al. 1992; He and Klionsky 2009; Boya et al. 2013). Studies in the past 10 years have shown that lipid droplets stored in liver cells under starvation conditions are wrapped by autophagosomes and fused to lysosomes via the endocytic system, where they are degraded to release ATP for mitochondria (Singh et al. 2009; Kaini et al. 2012; van Zutphen et al. 2014; Kaushik and Cuervo 2015). However, the molecular mechanism by which lipid droplets are targeted for autophagy has not yet been elucidated clearly.

The occurrence of autophagy is regulated by a variety of signaling pathways (He and Klionsky 2009; Lorzadeh et al. 2021). mTOR signaling is one of the most studied signaling pathways connected to the autophagy (Kamada et al. 2000; Hosokawa et al. 2009; Jung et al. 2009). mTOR pathway, which is negatively regulated by AMPK and cytoplasmic P53 signaling, inhibits autophagy activity (Ravikumar et al. 2010; Chang and Zou 2020). In addition to the abovementioned core regulatory network, autophagy is also regulated by other signaling, for example, Hh (Zeng and Ju 2018). Jimenez-Sanchez

et al. (2012) and Wang et al. (2013) showed that Hh signaling pathway inhibits autophagosome synthesis in HeLa and hepatocellular carcinoma cells respectively, while Pampliega et al. (2013) and Akhshi and Trimble (2021) indicate that the ciliary Hh signaling pathway induces autophagy in mouse embryonic fibroblasts (MEFs) and kidney epithelial cells. These contradictory results may be caused by different cell lines and the complexity of Hh signal transduction. Herein, we sought to explore the effects of Hh activation on autophagy and lipid metabolism in hepatocytes.

In this study, we show that Smo-binding small molecules, SAG and GDC-0449 but not SANT1 cause increased LC3 lipidation and elevated AMPK phosphorylation (P-AMPK) and upregulated lipid degradation, which can be blocked by knockdown of Smo rather than Sufu or Gli1, indicating that Hh signaling regulated autophagy and lipid metabolism through a non-canonical Smo signaling and Smo-AMPK axis.

Materials and methods

Cells and cell culture

AML12s were purchased from ATCC. AML12 cell lines were cultured in DMEM/F12 medium (HyClone) supplemented with 10% fetal bovine serum (FBS, Gibco, 10100154), 1× glutamine (Gibco, 35050061), and 1 mmol/L sodium pyruvate (Gibco, 11360070). MEF cells were cultured in DMEM medium supplemented with 10% FBS (Gibco).

Fatty acid preparation

Palmitic acid (PA; Sigma-Aldrich) and oleic acid (OA; Sigma-Aldrich) were dissolved in 10% fatty acid-free bovine serum albumin (BSA; Sigma-Aldrich). Stock solutions of PA and OA were further diluted with serum-free DMEM/F12 medium. Fifty micromole per liter oleic acid or 50 μmol/L FFA (oleic acid and palmitic acid mixed in a molar ratio of 2:1) was added to the serum-free DMEM/F12 medium overnight to establish an in vitro model of lipid accumulation in hepatocytes.

Transfection and siRNA

Cells were transfected with siRNA using lipofectamine RNAiMAX (Invitrogen), following the manufacturer's instructions. Cells were harvested after 48 h transfection for studies. ON-TARGETplus siRNA SMARTpool specific for the mouse Gli1, Smo, and Sufu were purchased from ThermoFisher.

RNA extraction and quantitative real-time PCR analyses

Total RNA was isolated from cultured cells using the RNAiso Plus reagent (TakaRa), and reverse transcription (RT) experiment was carried out using the HiScript II QRT SuperMix for quantitative (q)RT-PCR kit (Vazyme). RT-PCR was carried out using the AceQ qPCR SYBR Green Master Mix (Vazyme) on a RT-PCR system (Roche) with primers. The sequences of PCR primer pairs are: mouse Gli1 (GCTTGGATGAAGGACCTTGTG, GCTGATCCAGCCTAAGGTTCTC), mouse Ptc1(TGGCCGCATTGATCCCTATC, ACACAGGGGCTTGTGAAACA), mouse SREBP-1C(CACTTCTGGAGACATCGCAAAC,

ATGGTAGACAACAGCCGCATC), mouse SCD1(TCTTCCTTATCATTGCCAACACCA, GCGTTGAGCACCAGAGTGATATCG) mouse TNF-α(GTTCTATGGCCAGACCCTCAC, GGCACCACTAGTTGGTTGTCTTTG), and mouse HPRT (TATGGACAGGACTGAAAGAC, TAATCCAGCAGGTCAGCAAA). The expression levels of indicated genes were normalized to an internal control (HPRT), and the relative expression levels were evaluated using the $2^{-\Delta\Delta CT}$ method. Each target was measured in triplicate.

Western blotting

The indicated cells were washed twice with cold PBS and subsequently lysed in RIPA lysis buffer (150 mmol/L NaCl, 50 mmol/L Tris-HCl, pH 7.5, 1 mmol/L EDTA, pH 8.0, 0.5% sodium deoxycholate, 1% NP-40, 0.1% SDS, 2% sodium fluoride, and 0.5% sodium orthovanadate supplemented with protease inhibitor cocktail) at 4 °C for 30 min. After centrifugation to remove debris (14 000×g, 20 min), the protein concentration of each cell lysate sample was determined by the bicinchoninic acid assay. Each lysate was denatured in loading buffer at 95 °C for 5 min. Then, the lysates were resolved by 12% SDS-PAGE and transferred onto PVDF membranes. The membranes were blocked with 5% non-fat milk in TBST and probed with indicated primary antibodies followed by horseradish peroxidase-conjugated secondary antibodies (Jackson ImmunoResearch). Signals were visualized using Clarity Western ECL substrate (Bio-Rad). Densitometric analysis was carried out using ImageJ image analysis software.

Agonist and inhibitor

Cells were treated with SAG (0.5 μmol/L; Calbiochem), GDC-0449 (10 μmol/L; Selleck), GANT61 (20 μmol/L; Sigma), and SANT1 (50 μmol/L; Selleck) for a certain time. Then, cells were used for Western blotting, qRT-PCR, and BODIPY 493/503 staining assays.

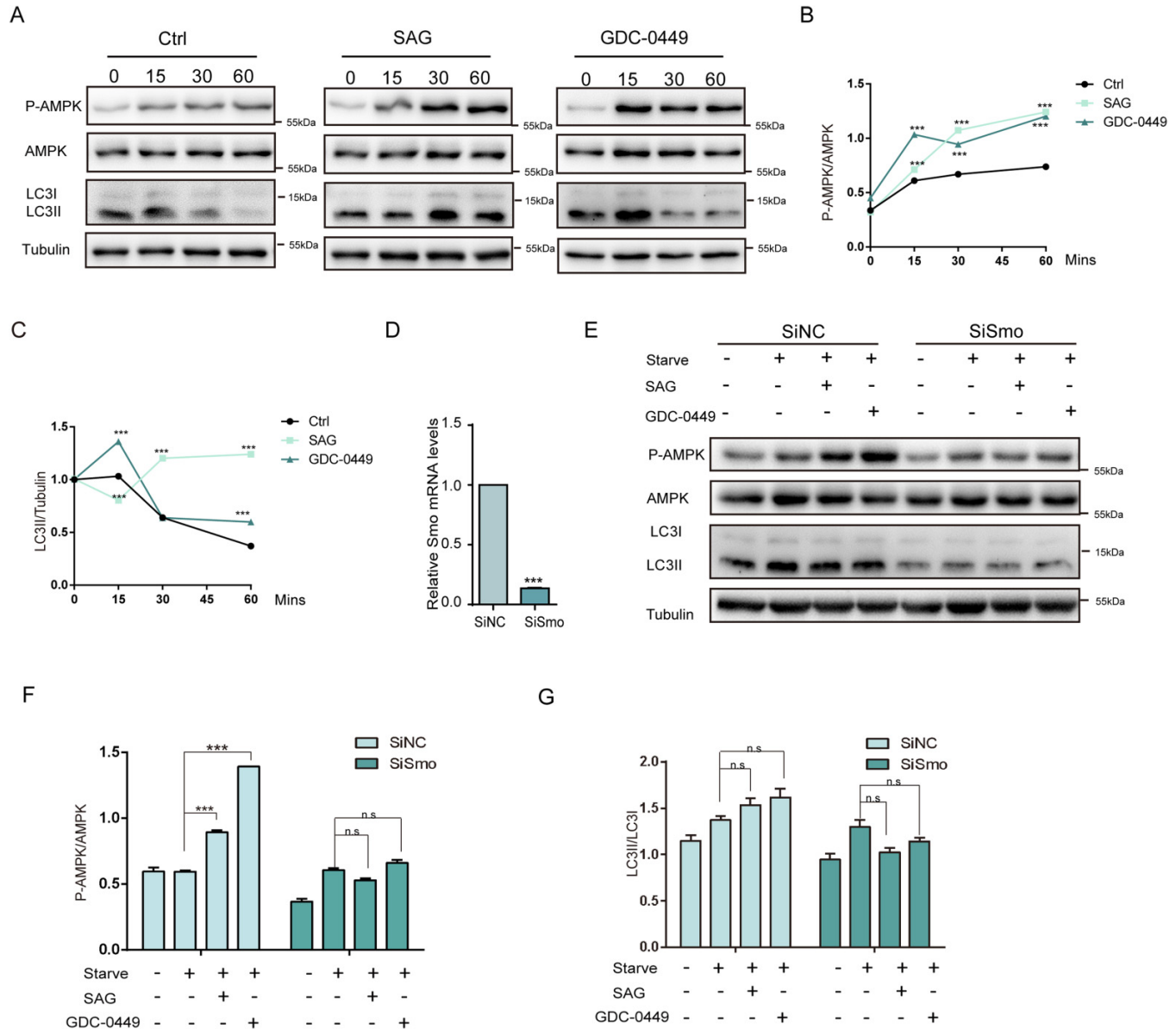
Fluorescence microscopy for BODIPY 493/503 (invitrogen)

AML12 cells were seeded on glasses and cultured with 50 μmol/L oleic acid or 50 μmol/L FFA overnight. Lipid droplets were stained by incubating cells with BODIPY 493/503 (Invitrogen), which was diluted with medium for 30 min in CO₂ incubator. Then, the cells were fixed with 4% paraformaldehyde and processed for immunofluorescence. Fluorescence-labeled lipid droplets were visualized with a Leica DMI3000 B microscope. Image-Pro Plus was used to calculate fluorescence area and cell number in each photo. The numbers of lipid droplets of different sizes were counted by limiting the pixel size. The staining area and the numbers of lipid droplets per cell were used as indicators.

Statistical analysis

Statistical analyses were performed using the GraphPad Prism Version 9.0 program. Data were presented as the mean ± SD. The difference between the two groups was analyzed using Student's *t* test. Multiple group comparisons were determined by one-way ANOVA with Tukey's post-hoc test. Each experiment was repeated at least three times. A *P* value

Fig. 1. Hedgehog activates AMPK via Smo to trigger autophagy in hepatocytes. (A) SAG and GDC-0449 were diluted in 0.5% FBS to treat AML12 cells for 0, 15, 30, and 60 min. P-AMPK, total AMPK, and LC3 were detected by Western blot. (B) Calculation of the pAMPK/AMPK ratio for each experimental group. (C) Calculation of the LC3-II/tubulin ratio for each experimental group. (D) RT-qPCR showed the efficiency of Smo knockdown. (E) P-AMPK and LC3-II were no longer upregulated with SAG or GDC-0449 treatment in the lack of Smo. (F) Calculation of the pAMPK/AMPK ratio for each experimental group. (G) Calculation of the LC3-II/LC3-I ratio for each experimental group. Each experiment was repeated at least three times. *** $P < 0.001$; ns, not significant.



less than 0.05 was interpreted to represent a statistically significant difference.

Results

Hh trigger autophagy via Smo-AMPK axis in hepatocytes

To examine the effect of Hh signal on autophagy in hepatocytes, we first treated the murine hepatocyte cells AML12 with either Smo agonist SAG or Smo inhibitor GDC-0449 and

measured LC3 conversion (LC3-I to LC3-II) by immunoblot analysis. Strikingly, the results showed that both SAG and GDC-0449 could upregulate the amount of LC3-II, a classical marker for autophagy (Figs. 1A-1C). In accordance with previous reports, although Smo modulators SAG and GDC-0449 had drastically different effects on the canonical Hh signaling, both of them could activate a non-canonical Smo-AMPK signaling cascades (Teperino et al. 2012). Thus, the dynamic changes of AMPK phosphorylation were detected within 1 h of stimulation. Compared with unstimulated cells, both SAG and GDC-0449 treatment caused a significant

Fig. 2. Canonical Hh signal transduction is absent in hepatocytes. (A) The transcriptional levels of *Gli1* and *Ptch1* in MEFs and (B) AML12, which were stimulated in different conditions were analyzed by RT-qPCR. (C) Colocalization of P-AMPK and Smo was examined during mitosis and cytokinesis. (D) Colocalization of P-AMPK and γ -tubulin was verified during mitosis and cytokinesis. (E) Calculation of the colocalization coefficients in (C) and (D) in AML12 cells. Each experiment was repeated at least three times. Around 5–10 cells were observed in each phase in Figs. 2C and 2D. ** $P < 0.01$, *** $P < 0.001$; ns, not significant.

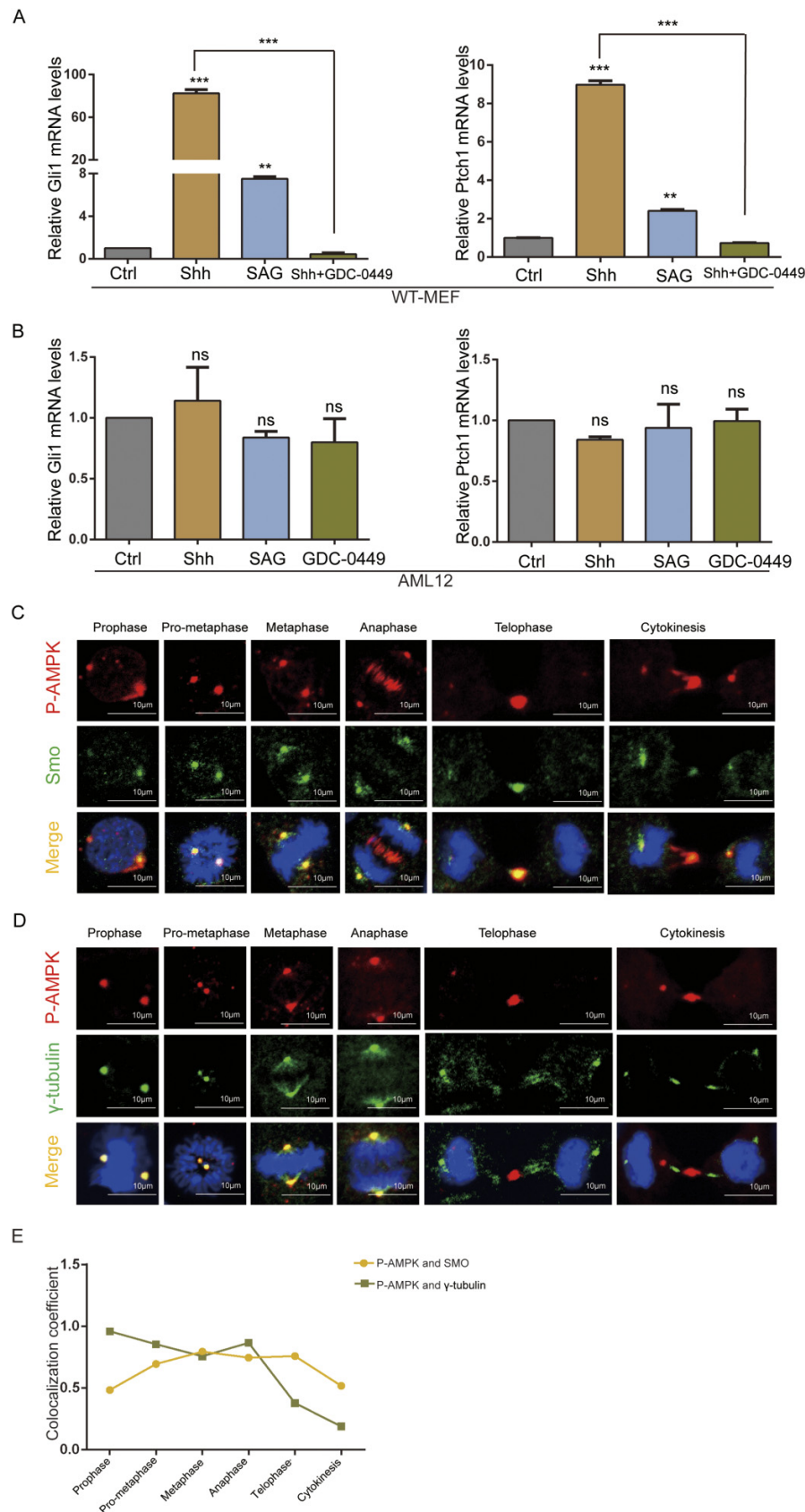


Fig. 3. SAG and GDC-0449 promote lipid degradation. AML12 cells were cultured in presence of 50 $\mu\text{mol/L}$ oleic acid and next day treated with SAG or GDC-0449 for 0, 6, 12, 18, and 24 h, respectively. (A) The neutral lipid stain BODIPY 493/503 was used to detect the morphological changes of LDs. (B) Quantification of these treated cells reveals the decreased average LD size by GDC-0449 but not SAG compared with control. (C) Number and average size of LDs were measured following imaging cells treated with SAG or GDC-0449. Each experiment was repeated at least three times. Around 250–300 cells were counted in different experimental groups. * $P < 0.05$; ** $P < 0.01$; *** $P < 0.001$.

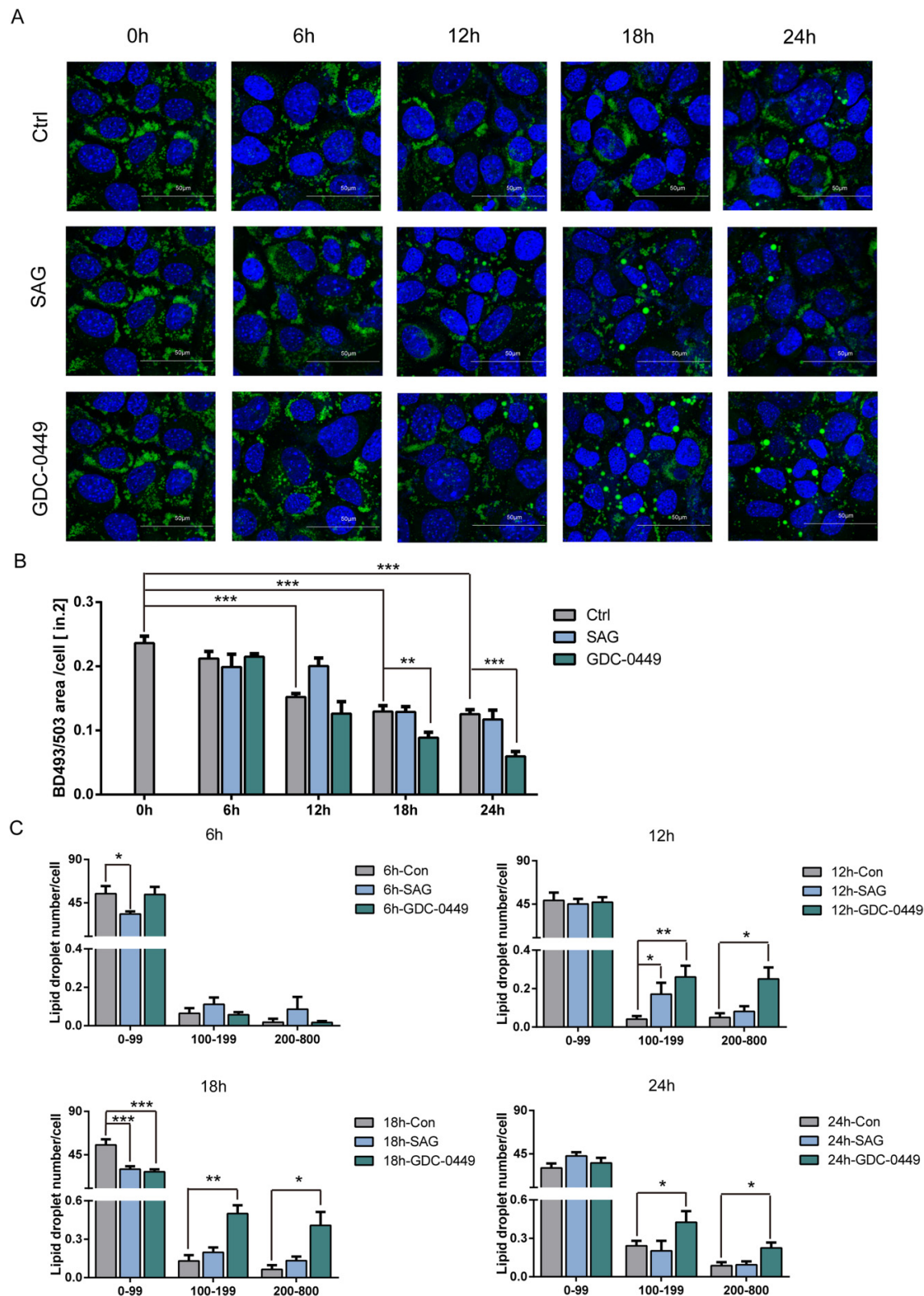
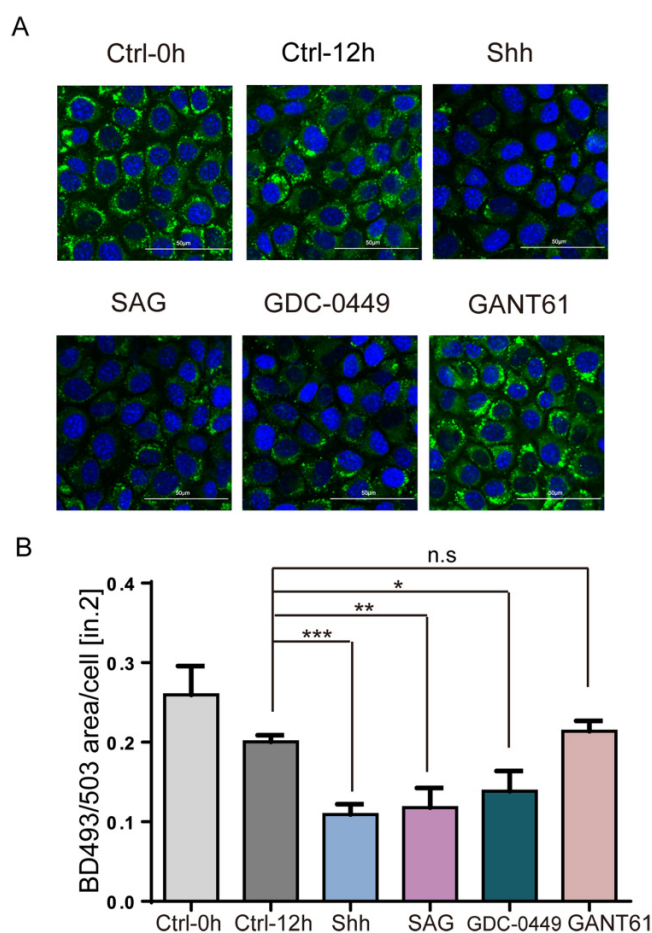


Fig. 4. Non-canonical Smo signal promotes lipid degradation. AML12 cells were cultured in presence of 50 $\mu\text{mol/L}$ FFA (oleic acid and palmitic acid mixed in a molar ratio of 2:1) and next day treated with Shh, SAG, GDC-0449, and GANT61 for 12 h, respectively. (A) BODIPY 493/503 was used to detect the morphological changes of LDs. (B) Quantification of these treated cells reveals the decreased average LD size by Shh, SAG, and GDC-0449 but not GANT61 compared with control. Each experiment was repeated at least three times. Around 250–300 cells were counted in different experimental groups. * $P < 0.05$; ** $P < 0.01$; *** $P < 0.001$; ns, not significant.



increase in AMPK phosphorylation, which could enhance autophagic activity through inhibiting the mTOR pathway as previously mentioned (Figs. 1A–1C). To further confirm the effect of Smo on autophagy and AMPK activity, Smo siRNA was transfected in AML12 cells. As expected, the level of P-AMPK and LC3-II was no longer elevated with SAG or GDC-0449 treatment because of a lack of Smo (Figs. 1D–1G). Taken together, our data indicated that Hh signaling activates AMPK via Smo to trigger autophagy in AML12 cells.

Canonical Hh signal transduction is absent in hepatocytes

It has been reported that hepatocytes do not assemble primary cilia, which are necessary for canonical Hh signal transduction (Seeley and Nachury 2010), and our previous results

from AML12 cell tests showed that non-canonical Smo signaling promotes autophagy through Smo–AMPK axis, suggesting that canonical Hh signal would be absent. To prove our hypothesis, we first evaluated the transcription response to Shh-conditioned medium (Shh-CM) or SAG or GDC-0449 stimulation in AML12 cells, respectively. RT-qPCR showed that no changes for Hh pathway target genes, including *Gli1* and *Ptch1*, were observed in AML12 cells, while with Hh ligand or SAG treatment, significant upregulation was detected in primary MEFs, which are sensitive to Hh signals, and dramatic reduction was also explored upon GDC-0449 stimulation, indicating that canonical Hh signal transduction is really not presence in hepatocytes (Figs. 2A and 2B).

Other groups previously demonstrated that Smo-induced AMPK activation requires Smo translocation to the cilium base where there is a special structure, called basal body (Teperino et al. 2012). Our results showed that although primary cilia were absent in the AML12 cells, Smo could also enhance AMPK phosphorylation (Figs. 1A–1G), further, P-AMPK and Smo concentrated at the centrosomes from prophase until anaphase and at the mid-body during telophase and cytokinesis by performing colocalization analyses of P-AMPK with Smo and γ -tubulin, respectively, thus suggesting that a centriole localization of Smo might be critical for activating AMPK, because both of basal body and centrosomes are composed of centrioles (Kobayashi and Dynlacht 2011) (Figs. 2C–2E).

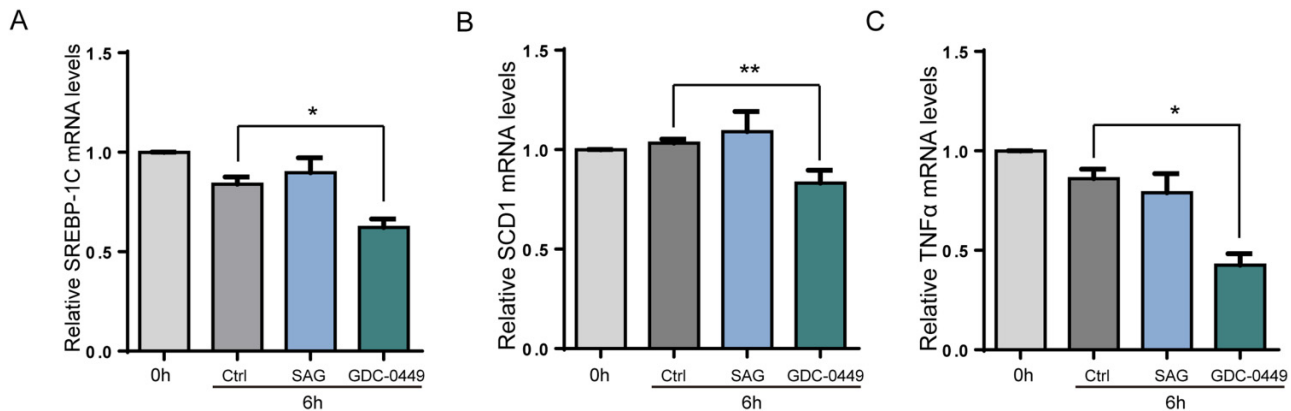
Non-canonical Smo signal promotes lipid degradation and suppresses lipogenesis in liver cells

The liver plays a key role in fat and energy metabolism. When energy is ingested in excess of needs, the fatty acids were stored as lipid droplets (LDs) composed of triglycerides in hepatocytes, while during nutrient starvation, there are two central processes to mediate the breakdown of LDs, lipolysis and autophagy (Singh et al. 2009; Qian et al. 2021). Based on the distinct changes in autophagic activity following SAG or GDC-0449 treatment in AML12 cells, we tested whether SAG or GDC-0449 regulates the lipid metabolism. As seen in confocal images and quantification in Figs. 3A and 3B, lipid staining with BODIPY 493/503 revealed decreased LD size in hepatocytes by addition of GDC-0449. However, unlike GDC-0449, SAG did not significantly affect the size of LDs (Figs. 3A and 3B). Of note, the number of larger-size LDs was dramatically increased in both SAG and GDC-0449 treatment groups at different time points, indicating that SAG and GDC-0449 promote lipid degradation in AML12 cells (Fig. 3C).

To extend these observations, we also tested the effect of Shh-CM and Gli inhibitor GANT-61 on LD morphology using AML12 cells treated for 12 h. As expected, Shh-CM or SAG, or GDC-0449 treatment caused a marked decrease in LD size compared with unstimulated cells, whereas significant alternation in Gli inhibitor GANT-61 was observed (Figs. 4A and 4B), indicating that inhibition of Shh downstream signal transduction did not affect fatty acid degradation.

Because activated AMPK has been linked to the down-regulation of sterol regulatory element-binding protein-1c

Fig. 5. SAG and GDC-0449 suppress lipogenesis. AML12 cells were cultured in presence of 50 $\mu\text{mol/L}$ oleic acid (OA) and next day treated with SAG or GDC-0449 for 6 h, respectively. (A) Fold changes in the mRNA levels of SREBP-1c, (B) SCD1, and (C) TNF α of the control, SAG, and GDC-0449-treated group were shown. Each experiment was repeated at least three times. * $P < 0.05$; ** $P < 0.01$.



(SREBP-1c), which executes the function of lipogenesis, we further assessed the effects of SAG and GDC-0449 on the expression of SREBP-1c (Li et al. 2011). RT-qPCR results revealed that GDC-0449 but not SAG reduced the mRNA levels of SREBP-1c (Fig. 5A). Consistent with the results of SREBP-1c, other genes involved in lipogenesis such as stearyl-CoA desaturase-1 (SCD1) and tumor necrosis factor alpha (TNF- α) were also suppressed upon treatment with GDC-0449 but not SAG in AML12 cells (Figs. 5B and 5C). Overall, these results indicate that non-canonical Smo signal plays a vital role during fat metabolism of lipid degradation and lipogenesis in liver cells.

Non-canonical Smo signal induced lipid degradation through SMO

As mentioned above, Smo modulator SAG and GDC-0449 could activate a non-canonical Smo signal that promotes lipid degradation in hepatocytes. To further verify the molecular mechanism of non-canonical Smo-regulated lipid metabolism, siRNAs were transfected to knock down Gli1, Smo, and Sufu, respectively in AML12 cells. The transfected cells were loaded with OA and chased for 18 h with serum-free medium to stimulate LD breakdown. The knockdown efficiency of siGli1, siSmo, and siSufu was validated by RT-qPCR (Fig. 6A), and lipid staining with BODIPY 493/503 revealed the decreased LD size and the increased number of larger-size LDs in both siGli1- and siSufu-treated cells with starvation, while siSmo showed the opposite results, indicating that LD breakdown enhanced by the Hh signaling pathway depends on Smo, rather than Gli1 and Sufu (Figs. 6B and 6C). These results confirm the findings of previous studies and establish that lipid degradation is regulated by non-canonical Smo pathway.

Discussion

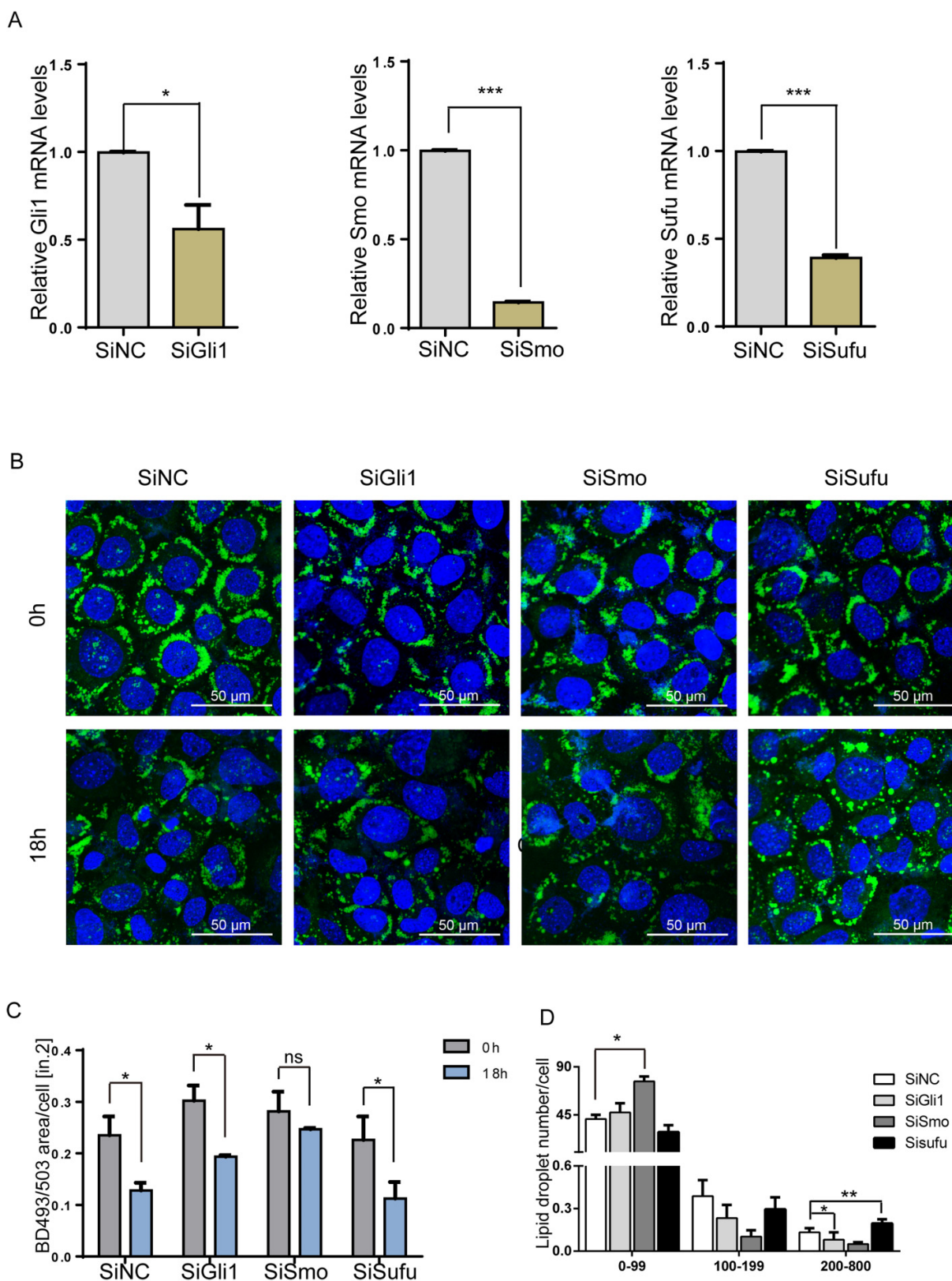
This study provides novel evidence that Hh signaling pathway is a key regulator of autophagy and lipid metabolism.

These results have been validated in mouse liver cells and confirmed at the steps of Smo in the non-canonical Hh pathway.

At first, we explored the regulation of Shh pathway on autophagy in AML12 cell lines. Although the Smo agonist SAG and antagonist GDC-0449 had opposite effect on the activity of the canonical Shh pathway, we were surprised that all of them caused the increase of AMPK phosphorylation and LC3-II in mouse liver cells. Since Shh signaling did not mediate the transcriptional activation of Smo-Gli in AML12 cells, it was considered that the non-canonical Smo signaling pathway was mainly involved in regulating autophagy. It required further investigation whether its regulation of P-AMPK was mediated by Smo or has other pharmacological effects. Therefore, we knocked down Smo in AML12 cells. The results showed that the elevated P-AMPK and LC3-II level by SAG and GDC-0449 was blocked by knockdown of Smo. So, it is suggested that Shh signal transduction activates AMPK phosphorylation that promotes autophagy by a Smo-dependent way.

Despite the clear effect of AMPK on autophagy, the role of its upstream activator Smo was less clear-cut. The non-canonical Smo-calcium/calmodulin-dependent protein kinase kinase 2 (Camkk2)-AMPK axis was originally identified in adipocytes, where it promoted a rapid metabolic rewiring toward glycolysis and increase of glucose uptake (Teperino et al. 2012). Moreover, Hh promotes polyamine biosynthesis in GCPs by engaging a non-canonical Hh/AMPK axis, leading to the translation of ornithine decarboxylase (D'Amico et al. 2015). Previous studies have also demonstrated that LKB1 and AMPK are located in the primary cilia, providing spatial evidence that Hh signal transduction may induce the activation of LKB1 and AMPK (Mick et al. 2015). In our study, we expanded these observations by demonstrating here that AMPK is indeed the integration point of Hh regulation on autophagy in hepatocytes. Considering that both of LKB1 and Camkk2 are AMPK upstream kinases, future work is certainly required to explore the relationship between Smo and both of them (Hardie 2011).

Fig. 6. Knockdown of *Smo* inhibits LD breakdown in liver cells. (A) The mRNA levels of *Gli1*, *Smo*, and *Sufu* in AML12 cells transfected with siRNAs were detected by RT-qPCR. (B) BODIPY 493/503 was used to detect the morphological changes of LDs. (C) Quantification of these transfected cells reveals the decreased average LD size by siNC, siGli1, and siSufu but not siSmo compared with control, respectively. (D) Number and average size of LDs were measured following imaging cells transfected with siRNAs. Each experiment was repeated at least three times. Around 250–300 cells were counted in different experimental groups. * $P < 0.05$; ** $P < 0.01$; *** $P < 0.001$; ns, not significant.



AMPK also plays an important role in regulating fat metabolism by rapidly engaging autophagy during acute starvation to maintain energy homeostasis (Hardie 2011). Therefore, the significance of SAG and GDC-0449 in the regulation of lipid metabolism was further examined. In liver cells, Shh-CM and SAG, and GDC-0449 promoted cell lipid degradation, while only GDC-0449 affected the lipogenesis, which may be the reason why there are fewer lipid droplets in GDC-0449-treated cells than in SAG-treated ones in Figs. 3A–3C. To explore the mechanism of Hh in regulating lipid metabolism, we knocked down *Gli1*, *Smo*, and *Sufu*, respectively to detect LD breakdown during starvation. The results showed that knockdown of *Smo* rather than *Gli1* or *Sufu* inhibited the LD breakdown in AML12 cells. This discovery is also consistent with previous research.

Excessive fat accumulation and subsequent formation of LDs in hepatocytes contribute to hepatic steatosis and non-alcoholic steatohepatitis, which is extremely harmful to human health, so scientists have paid great attention to the research on autophagy degradation of LDs in the past 10 years (Roberts and Olzmann 2020; Rakotonirina-Ricquebourg et al. 2022). Here, we identified that SAG and GDC-0449 promote autophagy and lipid degradation in hepatocytes, suggesting that *Smo* is likely to be as a potential druggable molecular target for lessening the impact of abnormal lipid accumulation. In other words, increasing the activity of a non-canonical *Smo* pathway, *Smo*–AMPK axis may provide a new approach to prevent metabolic syndrome and its associated pathologies.

Article information

History dates

Received: 14 November 2022

Accepted: 7 February 2023

Accepted manuscript online: 23 February 2023

Version of record online: 27 March 2023

Copyright

© 2023 The Author(s). Permission for reuse (free in most cases) can be obtained from [creativecommons.org](https://creativecommons.org/licenses/by/4.0/).

Data availability

Data generated or analyzed during this study are provided in full within the published article.

Author information

Author ORCIDs

Chen Liu <https://orcid.org/0000-0002-7134-4367>

Author notes

Yixing Yao, Tianyuan Li, and Tingting Yu contributed equally to this work.

Author contributions

Conceptualization: CL, SY

Data curation: YY, TL, CL, SY

Formal analysis: YY, TL, XY, CL, SY

Funding acquisition: TY, SYC, CL, SY

Investigation: YY, TY, XY, CL

Methodology: YY, TY, CL

Project administration: SYC, CL, SY

Resources: YY, TY, CL, SY

Software: YY, TY, YW, SY

Supervision: CL, SY

Validation: YY, TL, CL, SY

Visualization: TY, JC, SYC, SY

Writing – original draft: YY, CL

Writing – review & editing: SYC, CL, SY

Competing interests

The authors declare that they have no conflicts of interest with the contents of this article.

Funding information

This work was supported by grants from the Chinese National Science Foundation (82173291 to SY, 81702747 to CL, and 81871936 and 82172629 to SYC).

References

- Akhshi, T., and Trimble, W.S. 2021. A non-canonical Hedgehog pathway initiates ciliogenesis and autophagy. *J. Cell Biol.* **220**. doi:[10.1083/jcb.202004179](https://doi.org/10.1083/jcb.202004179). PMID: [33258871](https://pubmed.ncbi.nlm.nih.gov/33258871/).
- Boya, P., Reggiori, F., and Codogno, P. 2013. Emerging regulation and functions of autophagy. *Nat. Cell Biol.* **15**: 713–720. doi:[10.1038/ncb2788](https://doi.org/10.1038/ncb2788). PMID: [23817233](https://pubmed.ncbi.nlm.nih.gov/23817233/).
- Chang, H., and Zou, Z. 2020. Targeting autophagy to overcome drug resistance: further developments. *J. Hematol. Oncol.* **13**: 159. doi:[10.1186/s13045-020-01000-2](https://doi.org/10.1186/s13045-020-01000-2). PMID: [33239065](https://pubmed.ncbi.nlm.nih.gov/33239065/).
- Corbit, K.C., Aanstad, P., Singla, V., Norman, A.R., Stainier, D.Y.R., and Reiter, J.F. 2005. Vertebrate Smoothed functions at the primary cilium. *Nature*, **437**: 1018–1021. doi:[10.1038/nature04117](https://doi.org/10.1038/nature04117). PMID: [16136078](https://pubmed.ncbi.nlm.nih.gov/16136078/).
- D'Amico, D., Antonucci, L., Di Magno, L., Coni, S., Sdruscia, G., Macone, A., et al. 2015. Non-canonical Hedgehog/AMPK-mediated control of polyamine metabolism supports neuronal and medulloblastoma cell growth. *Dev. Cell*, **35**: 21–35. doi:[10.1016/j.devcel.2015.09.008](https://doi.org/10.1016/j.devcel.2015.09.008). PMID: [26460945](https://pubmed.ncbi.nlm.nih.gov/26460945/).
- Falkenstein, K.N., and Vokes, S.A. 2014. Transcriptional regulation of graded Hedgehog signaling. *Semin. Cell Dev. Biol.* **33**: 73–80. doi:[10.1016/j.semcdb.2014.05.010](https://doi.org/10.1016/j.semcdb.2014.05.010).
- Hardie, D.G. 2011. AMP-activated protein kinase—an energy sensor that regulates all aspects of cell function. *Genes Dev.* **25**: 1895–1908. doi:[10.1101/gad.17420111](https://doi.org/10.1101/gad.17420111).
- He, C., and Klionsky, D.J. 2009. Regulation mechanisms and signaling pathways of autophagy. *Annu. Rev. Genet.* **43**: 67–93. doi:[10.1146/annurev-genet-102808-114910](https://doi.org/10.1146/annurev-genet-102808-114910).
- Hosokawa, N., Hara, T., Kaizuka, T., Kishi, C., Takamura, A., Miura, Y., et al. 2009. Nutrient-dependent mTORC1 association with the ULK1-Atg13-FIP200 complex required for autophagy. *Mol. Biol. Cell*, **20**: 1981–1991. doi:[10.1091/mbc.E08-12-1248](https://doi.org/10.1091/mbc.E08-12-1248).
- Ingham, P.W., and McMahon, A.P. 2001. Hedgehog signaling in animal development: paradigms and principles. *Genes Dev.* **15**: 3059–3087. doi:[10.1101/gad.938601](https://doi.org/10.1101/gad.938601).
- Ingham, P.W., Nakano, Y., and Seger, C. 2011. Mechanisms and functions of Hedgehog signalling across the metazoa. *Nat. Rev. Genet.* **12**: 393–406. doi:[10.1038/nrg2984](https://doi.org/10.1038/nrg2984).
- Jiang, J., and Hui, C.C. 2008. Hedgehog signaling in development and cancer. *Dev. Cell*, **15**: 801–812. doi:[10.1016/j.devcel.2008.11.010](https://doi.org/10.1016/j.devcel.2008.11.010).
- Jimenez-Sanchez, M., Menzies, F.M., Chang, Y.Y., Simecek, N., Neufeld, T.P., and Rubinsztein, D.C. 2012. The Hedgehog signalling pathway regulates autophagy. *Nat. Commun.* **3**: 1200. doi:[10.1038/ncomms2212](https://doi.org/10.1038/ncomms2212).

- Jung, C.H., Jun, C.B., Ro, S.H., Kim, Y.M., Otto, N.M., Cao, J., et al. 2009. ULK-Atg13-FIP200 complexes mediate mTOR signaling to the autophagy machinery. *Mol. Biol. Cell*, **20**: 1992–2003. doi:[10.1091/mbc.E08-12-1249](https://doi.org/10.1091/mbc.E08-12-1249).
- Kaini, R.R., Sillerud, L.O., Zhaorigetu, S., and Hu, C.A.A. 2012. Autophagy regulates lipolysis and cell survival through lipid droplet degradation in androgen-sensitive prostate cancer cells. *Prostate*, **72**: 1412–1422. doi:[10.1002/pros.22489](https://doi.org/10.1002/pros.22489).
- Kamada, Y., Funakoshi, T., Shintani, T., Nagano, K., Ohsumi, M., and Ohsumi, Y. 2000. Tor-mediated induction of autophagy via an Apg1 protein kinase complex. *J. Cell Biol.* **150**: 1507–1513. doi:[10.1083/jcb.150.6.1507](https://doi.org/10.1083/jcb.150.6.1507).
- Kaushik, S., and Cuervo, A.M. 2015. Degradation of lipid droplet-associated proteins by chaperone-mediated autophagy facilitates lipolysis. *Nat. Cell Biol.* **17**: 759–770. doi:[10.1038/ncb3166](https://doi.org/10.1038/ncb3166).
- Kinzler, K.W., Ruppert, J.M., Bigner, S.H., and Vogelstein, B. 1988. The *GLI* gene is a member of the *Kruppel* family of zinc finger proteins. *Nature*, **332**: 371–374. doi:[10.1038/332371a0](https://doi.org/10.1038/332371a0).
- Kobayashi, T., and Dynlacht, B.D. 2011. Regulating the transition from centriole to basal body. *J. Cell Biol.* **193**: 435–444. doi:[10.1083/jcb.201101005](https://doi.org/10.1083/jcb.201101005).
- Li, Y., Xu, S., Mihaylova, M.M., Zheng, B., Hou, X., Jiang, B., et al. 2011. AMPK phosphorylates and inhibits SREBP activity to attenuate hepatic steatosis and atherosclerosis in diet-induced insulin-resistant mice. *Cell Metab.* **13**: 376–388. doi:[10.1016/j.cmet.2011.03.009](https://doi.org/10.1016/j.cmet.2011.03.009).
- Lorzadeh, S., Kohan, L., Ghavami, S., and Azarpira, N. 2021. Autophagy and the Wnt signaling pathway: a focus on Wnt/beta-catenin signaling. *Biochim. Biophys. Acta Mol. Cell Res.* **1868**: 118926. doi:[10.1016/j.bbamcr.2020.118926](https://doi.org/10.1016/j.bbamcr.2020.118926).
- Lum, L., and Beachy, P.A. 2004. The Hedgehog response network: sensors, switches, and routers. *Science*, **304**: 1755–1759. doi:[10.1126/science.1098020](https://doi.org/10.1126/science.1098020).
- Mick, D.U., Rodrigues, R.B., Leib, R.D., Adams, C.M., Chien, A.S., Gygi, S.P., and Nachury, M.V. 2015. Proteomics of primary cilia by proximity labeling. *Dev. Cell*, **35**: 497–512. doi:[10.1016/j.devcel.2015.10.015](https://doi.org/10.1016/j.devcel.2015.10.015).
- Nusslein-Volhard, C., and Wieschaus, E. 1980. Mutations affecting segment number and polarity in *Drosophila*. *Nature*, **287**: 795–801. doi:[10.1038/287795a0](https://doi.org/10.1038/287795a0).
- Pampliega, O., Orhon, I., Patel, B., Sridhar, S., Diaz-Carretero, A., Beau, I., et al. 2013. Functional interaction between autophagy and ciliogenesis. *Nature*, **502**: 194–200. doi:[10.1038/nature12639](https://doi.org/10.1038/nature12639).
- Praktiknjo, S.D., Saad, F., Maier, D., Ip, P., and Hipfner, D.R. 2018. Activation of Smoothened in the Hedgehog pathway unexpectedly increases Galphas-dependent cAMP levels in *Drosophila*. *J. Biol. Chem.* **293**: 13496–13508. doi:[10.1074/jbc.RA118.001953](https://doi.org/10.1074/jbc.RA118.001953).
- Qian, H., Chao, X., Williams, J., Fulte, S., Li, T., Yang, L., and Ding, W.X. 2021. Autophagy in liver diseases: a review. *Mol. Aspects Med.* **82**: 100973. doi:[10.1016/j.mam.2021.100973](https://doi.org/10.1016/j.mam.2021.100973).
- Qu, C., Liu, Y., Kunkalla, K., Singh, R.R., Blonska, M., Lin, X., et al. 2013. Trimeric G protein-CARMA1 axis links smoothened, the hedgehog receptor transducer, to NF-kappaB activation in diffuse large B-cell lymphoma. *Blood*, **121**: 4718–4728. doi:[10.1182/blood-2012-12-470153](https://doi.org/10.1182/blood-2012-12-470153).
- Rakotonirina-Ricquebourg, R., Costa, V., and Teixeira, V. 2022. Hello from the other side: membrane contact of lipid droplets with other organelles and subsequent functional implications. *Prog. Lipid Res.* **85**: 101141. doi:[10.1016/j.plipres.2021.101141](https://doi.org/10.1016/j.plipres.2021.101141).
- Ravikumar, B., Sarkar, S., Davies, J.E., Futter, M., Garcia-Arencibia, M., Green-Thompson, Z.W., et al. 2010. Regulation of mammalian autophagy in physiology and pathophysiology. *Physiol. Rev.* **90**: 1383–1435. doi:[10.1152/physrev.00030.2009](https://doi.org/10.1152/physrev.00030.2009).
- Riobo, N.A., Saucy, B., Dilizio, C., and Manning, D.R. 2006. Activation of heterotrimeric G proteins by Smoothened. *Proc. Natl. Acad. Sci. U.S.A.* **103**: 12607–12612. doi:[10.1073/pnas.0600880103](https://doi.org/10.1073/pnas.0600880103).
- Roberts, M.A., and Olzmann, J.A. 2020. Protein quality control and lipid droplet metabolism. *Annu. Rev. Cell Dev. Biol.* **36**: 115–139. doi:[10.1146/annurev-cellbio-031320-101827](https://doi.org/10.1146/annurev-cellbio-031320-101827).
- Rohatgi, R., Milenkovic, L., and Scott, M.P. 2007. Patched1 regulates Hedgehog signaling at the primary cilium. *Science*, **317**: 372–376. doi:[10.1126/science.1139740](https://doi.org/10.1126/science.1139740).
- Seeley, E.S., and Nachury, M.V. 2010. The perennial organelle: assembly and disassembly of the primary cilium. *J. Cell Sci.* **123**: 511–518. doi:[10.1242/jcs.061093](https://doi.org/10.1242/jcs.061093).
- Singh, R., Kaushik, S., Wang, Y., Xiang, Y., Novak, I., Komatsu, M., et al. 2009. Autophagy regulates lipid metabolism. *Nature*, **458**: 1131–1135. doi:[10.1038/nature07976](https://doi.org/10.1038/nature07976).
- Takeshige, K., Baba, M., Tsuboi, S., Noda, T., and Ohsumi, Y. 1992. Autophagy in yeast demonstrated with proteinase-deficient mutants and conditions for its induction. *J. Cell Biol.* **119**: 301–311. doi:[10.1083/jcb.119.2.301](https://doi.org/10.1083/jcb.119.2.301).
- Teperino, R., Amann, S., Bayer, M., Mcgee, S.L., Loipetzberger, A., Connor, T., et al. 2012. Hedgehog partial agonism drives Warburg-like metabolism in muscle and brown fat. *Cell*, **151**: 414–426. doi:[10.1016/j.cell.2012.09.021](https://doi.org/10.1016/j.cell.2012.09.021).
- van Zutphen, T., Todde, V., de Boer, R., Kreim, M., Hofbauer, H.F., Wolinski, H., et al. 2014. Lipid droplet autophagy in the yeast *Saccharomyces cerevisiae*. *Mol. Biol. Cell*, **25**: 290–301. doi:[10.1091/mbc.E13-08-0448](https://doi.org/10.1091/mbc.E13-08-0448).
- Wang, Y., Han, C., Lu, L., Magliato, S., and Wu, T. 2013. Hedgehog signaling pathway regulates autophagy in human hepatocellular carcinoma cells. *Hepatology*, **58**: 995–1010. doi:[10.1002/hep.26394](https://doi.org/10.1002/hep.26394).
- Zeng, X., and Ju, D. 2018. Hedgehog signaling pathway and autophagy in cancer. *Int. J. Mol. Sci.* **19**. doi:[10.3390/ijms19082279](https://doi.org/10.3390/ijms19082279).